Appendix A1 – Heating Degree Day Model

Least Squares Regressional Analysis

Qualitative assessment of the provided heating degree day and temperature data from the nine selected climate models gave the impression of two important characteristics:

1) A linearly decreasing trend of the HDD
2) A periodic, approximately sinusoidal trend

As such, the following model, a combination of a linear trend and a four term Fourier series approximation, was selected to represent the heating degree day data. It was qualitatively assessed by the use of the built in excel solver that including more terms in the Fourier series approximation would not significantly increase the model accuracy.

$\hat{y} = a_{01} + a_{02}t + a_1\cos(\omega_0 t) + b_1\sin(\omega_0 t) + a_2\cos(2\omega_0 t) + b_2\sin(2\omega_0 t) + a_3\cos(3\omega_0 t) + b_3\sin(3\omega_0 t) + a_4\cos(4\omega_0 t) + b_4\sin(4\omega_0 t)$

For all further equations, we will use the following short form notation for each of the sine and cosine functions

$c_1 = \cos(\omega_0 t), c_2 = \cos(2\omega_0 t), c_3 = \cos(3\omega_0 t), c_4 = \cos(4\omega_0 t)$
$s_1 = \sin(\omega_0 t), s_2 = \sin(2\omega_0 t), s_3 = \sin(3\omega_0 t), s_4 = \sin(4\omega_0 t)$

Therefore

$\hat{y} = a_{01} + a_{02}t + a_1c_1 + b_1s_1 + a_2c_2 + b_2s_2 + a_3c_3 + b_3s_3 + a_4c_4 + b_4s_4$

The regression coefficients of this model were then determined by evaluating the least squares sum in the following six steps:

1) Expansion of the sum

$$S_r = \sum_{i=1}^{n}(y_i - \hat{y}_i)^2$$

$$S_r = \sum_{i=1}^{n}\left(y_i - (a_{01} + a_{02}t + a_1c_1 + b_1s_1 + a_2c_2 + b_2s_2 + a_3c_3 + b_3s_3 + a_4c_4 + b_4s_4)\right)^2$$

2) Partial derivation of the least squares sum with respect to each of the regression coefficients, and minimization of each derivative

$$\frac{\partial S_r}{\partial a_{01}} = -2\sum(y_i - \hat{y}_i) = 0 \qquad \frac{\partial S_r}{\partial a_{02}} = -2\sum(y_i - \hat{y}_i)t_i = 0$$

$$\frac{\partial S_r}{\partial a_1} = -2\sum(y_i - \hat{y}_i)c_1 = 0 \qquad \frac{\partial S_r}{\partial b_1} = -2\sum(y_i - \hat{y}_i)s_1 = 0$$

$$\frac{\partial S_r}{\partial a_2} = -2\sum(y_i - \hat{y}_i)c_2 = 0 \qquad \frac{\partial S_r}{\partial b_2} = -2\sum(y_i - \hat{y}_i)s_2 = 0$$

$$\frac{\partial S_r}{\partial a_3} = -2\sum(y_i - \hat{y}_i)c_3 = 0 \qquad \frac{\partial S_r}{\partial b_3} = -2\sum(y_i - \hat{y}_i)s_3 = 0$$

$$\frac{\partial S_r}{\partial a_4} = -2\sum(y_i - \hat{y}_i)c_4 = 0 \qquad \frac{\partial S_r}{\partial b_4} = -2\sum(y_i - \hat{y}_i)s_4 = 0$$

3) Expansion of the minima equations into matrix form

$$\begin{bmatrix} N & \sum t & \sum c_1 & \sum s_1 & \sum c_2 & \sum s_2 & \sum c_3 & \sum s_3 & \sum c_4 & \sum s_4 \\ \sum t & \sum t^2 & \sum tc_1 & \sum ts_1 & \sum tc_2 & \sum ts_2 & \sum tc_3 & \sum ts_3 & \sum tc_4 & \sum ts_4 \\ \sum c_1 & \sum tc_1 & \sum {c_1}^2 & \sum c_1s_1 & \sum c_1c_2 & \sum c_1s_2 & \sum c_1c_3 & \sum c_1s_3 & \sum c_1c_4 & \sum c_1s_4 \\ \sum s_1 & \sum ts_1 & \sum c_1s_1 & \sum {s_1}^2 & \sum s_1c_2 & \sum s_1s_2 & \sum s_1c_3 & \sum s_1s_3 & \sum s_1c_4 & \sum s_1s_4 \\ \sum c_2 & \sum tc_2 & \sum c_1c_2 & \sum s_1c_2 & \sum {c_2}^2 & \sum c_2s_2 & \sum c_2c_3 & \sum c_2s_3 & \sum c_2c_4 & \sum c_2s_4 \\ \sum s_2 & \sum ts_2 & \sum c_1s_2 & \sum s_1s_2 & \sum c_2s_2 & \sum {s_2}^2 & \sum s_2c_3 & \sum s_2s_3 & \sum s_2c_4 & \sum s_2s_4 \\ \sum c_3 & \sum tc_3 & \sum c_1c_3 & \sum s_1c_3 & \sum c_2c_3 & \sum s_2c_3 & \sum {c_3}^2 & \sum c_3s_3 & \sum c_3c_4 & \sum c_3s_4 \\ \sum s_3 & \sum ts_3 & \sum c_1s_3 & \sum s_1s_3 & \sum c_2s_3 & \sum s_2s_3 & \sum c_3s_3 & \sum {s_3}^2 & \sum s_3c_4 & \sum s_3s_4 \\ \sum c_4 & \sum tc_4 & \sum c_1c_4 & \sum s_1c_4 & \sum c_2c_4 & \sum s_2c_4 & \sum c_3c_4 & \sum s_3c_4 & \sum {c_4}^2 & \sum c_4s_4 \\ \sum s_4 & \sum ts_4 & \sum c_1s_4 & \sum s_1s_4 & \sum c_2s_4 & \sum s_2s_4 & \sum c_3s_4 & \sum s_3s_4 & \sum c_4s_4 & \sum {s_4}^2 \end{bmatrix} \begin{bmatrix} a_{01} \\ a_{02} \\ a_1 \\ b_1 \\ a_2 \\ b_2 \\ a_3 \\ b_3 \\ a_4 \\ b_4 \end{bmatrix} = \begin{bmatrix} \sum y \\ \sum yt \\ \sum yc_1 \\ \sum ys_1 \\ \sum yc_2 \\ \sum ys_2 \\ \sum yc_3 \\ \sum ys_3 \\ \sum yc_4 \\ \sum ys_4 \end{bmatrix}$$

4) Simplification of the matrix using the following techniques to result in the following
   a. The average of a sinusoidal function centered about zero over a complete number of periods is 0.
   b. The average of a squared sinusoidal function over a complete set of periods is N/2.
   c. The use of partial sum formulas

$$\sum_{i=1}^{n} t_i = \frac{1}{2}N(N+1)$$

$$\sum_{i=1}^{n} {t_i}^2 = \frac{1}{6}N(N+1)(2N+1)$$

$$\begin{bmatrix} N & \frac{1}{2}N(N+1) & 0 & 0 & 0 & 0 & 0 & 0 & 0 & 0 \\ \frac{1}{2}N(N+1) & \frac{1}{6}N(N+1)(2N+1) & \frac{N}{2} & \sum ts_1 & \frac{N}{2} & \sum ts_2 & \frac{N}{2} & \sum ts_3 & \frac{N}{2} & \sum ts_4 \\ 0 & \frac{N}{2} & \frac{N}{2} & 0 & 0 & 0 & 0 & 0 & 0 & 0 \\ 0 & \sum ts_1 & 0 & \frac{N}{2} & 0 & 0 & 0 & 0 & 0 & 0 \\ 0 & \frac{N}{2} & 0 & 0 & \frac{N}{2} & 0 & 0 & 0 & 0 & 0 \\ 0 & \sum ts_2 & 0 & 0 & 0 & \frac{N}{2} & 0 & 0 & 0 & 0 \\ 0 & \frac{N}{2} & 0 & 0 & 0 & 0 & \frac{N}{2} & 0 & 0 & 0 \\ 0 & \sum ts_3 & 0 & 0 & 0 & 0 & 0 & \frac{N}{2} & 0 & 0 \\ 0 & \frac{N}{2} & 0 & 0 & 0 & 0 & 0 & 0 & \frac{N}{2} & 0 \\ 0 & \sum ts_4 & 0 & 0 & 0 & 0 & 0 & 0 & 0 & \frac{N}{2} \end{bmatrix} \begin{bmatrix} a_{01} \\ a_{02} \\ a_1 \\ b_1 \\ a_2 \\ b_2 \\ a_3 \\ b_3 \\ a_4 \\ b_4 \end{bmatrix} = \begin{bmatrix} \sum y \\ \sum yt \\ \sum yc_1 \\ \sum ys_1 \\ \sum yc_2 \\ \sum ys_2 \\ \sum yc_3 \\ \sum ys_3 \\ \sum yc_4 \\ \sum ys_4 \end{bmatrix}$$

5) Matrix row reduction to result in the following solution for each of the regression coefficients

$$a_{02} = \frac{-\frac{1}{2}(N+1)\sum y + \sum yt - \sum yc_1 - \frac{2}{N}\sum ts_1 \sum ys_1 - \sum yc_2 - \frac{2}{N}\sum ts_2 \sum ys_2 - \sum yc_3 - \frac{2}{N}\sum ts_3 \sum ys_3 - \sum yc_4 - \frac{2}{N}\sum ts_4 \sum ys_4}{\frac{1}{6}N(N+1)(2N+1) - \frac{1}{4}N(N+1) - \frac{2}{N}(\sum ts_1)^2 - \frac{2}{N}(\sum ts_2)^2 - \frac{2}{N}(\sum ts_3)^2 - \frac{2}{N}(\sum ts_4)^2 - 2N}$$

$$a_{01} = \frac{\sum y}{N} - \frac{1}{2}(N+1)a_{02}$$

$$a_1 = \frac{2}{N}\sum yc_1 - a_{02}$$

$$b_1 = \frac{2}{N}\sum ys_1 - \frac{2}{N}\left(\sum ts_1\right)a_{02}$$

$$a_2 = \frac{2}{N}\sum yc_2 - a_{02}$$

$$b_2 = \frac{2}{N}\sum ys_2 - \frac{2}{N}\left(\sum ts_2\right)a_{02}$$

$$a_3 = \frac{2}{N}\sum yc_3 - a_{02}$$

$$b_3 = \frac{2}{N}\sum ys_3 - \frac{2}{N}\left(\sum ts_3\right)a_{02}$$

$$a_4 = \frac{2}{N}\sum yc_4 - a_{02}$$
$$b_4 = \frac{2}{N}\sum ys_4 - \frac{2}{N}\left(\sum ts_4\right)a_{02}$$

6) Numerical solutions to any remaining summations which could not be simplified and numerical calculation of the regression coefficients.

A quadratic regression model was then used to determine an upper and lower bound of each heating degree day and temperature model. The residuals were sorted in ascending order using the ranking and vlookup functions in excel. The x-axis of the residual plot, the predicted heating degree day or temperature of the model, was then rounded to provide a series of non-unique data points. This rounding allowed the minimum and maximum residual points to be determined, thus eliminating the data points that would otherwise prevent the correct bounding of the residual plot. Without rounding, nearly all data points were unique, and thus all data points would be included in any bounding curve calculation. By increasing or decreasing the rounded decimal point the tightness of the bounding could be decreased or increased, respectively. The following equations were used to calculate the bounding quadratic equations using the minimum or maximum residual values. The resulting maximum and minimum residual predictions were then added to the heating degree day or temperature model to provide upper and lower predictions:

$$g(x) = ax^2 + bx + c$$
$$let\ x = \hat{y}, z = \hat{y} - y, where\ z_{max}\ or\ z_{min}\ are\ used$$
$$a = \frac{S(x^2z) * S(xx) - S(xz) * S(xx^2)}{S(xx) * S(x^2x^2) - S(xx^2)^2}$$
$$b = \frac{S(xz) * S(x^2x^2) - S(x^2z) * S(xx^2)}{S(xx) * S(x^2x^2) - S(xx^2)^2}$$
$$c = \frac{\sum z_i}{n} - b * \frac{\sum x_i}{n} - a * \frac{\sum {x_i}^2}{n}$$
$$S(xx) = \sum {x_i}^2 - \frac{(\sum x_i)^2}{n}, \qquad S(xz) = \sum x_i z_i - \frac{\sum x_i \sum z_i}{n}$$
$$S(xx^2) = \sum {x_i}^3 - \frac{\sum x_i (\sum x_i)^2}{n}, \qquad S(x^2z) = \sum {x_i}^2 z_i - \frac{(\sum x_i)^2 \sum z_i}{n}$$
$$S(x^2x^2) = \sum {x_i}^4 - \frac{(\sum {x_i}^2)^2}{n}$$

Table 1 and Table 2, given below provide the heating degree day and temperature regression coefficients of each of the selected models. The model selections were made by OURANOS for the 10th, 50th, & 90th percentiles for the 2030 (2011-2040), the 2050 (2041-2070), & the 2080 (2071-2100) normals. The R^2 coefficients of the models have also been provided as a measure of model suitability. To validate the accuracy of the models, each model was compared against both the observed historical data [1], and the gridded historical data [2], as shown by the calculated R^2 values provided. Furthermore, the coefficients for the predicted upper and lower bounding quadratic equations are provided. Graphs of the models and their residuals are provided in Figure 1 through Figure 36.

As can be seen in both the partial plots and the residual plots, the greatest variation of the model from the climate model heating degree day values occurs in the winter months, where the predicted value is greatest. While this could be seen as a failure of the model to accurately predict the heating degree days in the winter season, it is commonplace to see large variations in temperature, and thus heating degree days, in the winter season. Additionally, the total heating degree day for the climate normal was identical to the modeled data.

Table 1 – Heating Degree Day Regression Coefficients

Model Coefficient	Historical (1971-2000)		2030 (2011-2040)			2050 (2041-2070)			2080 (2071-2100)		
	NRCan Gridded	Whitehorse A	MRI-CGCM3 rcp26_r1i1p1	CNRM-CM5 rcp85_r1i1p1	CanESM2G rcp85_r1i1p1	GFDL-ESM2G rcp26_r1i1p1	CCSM4 rcp26_r2i1p1	HadGEM2-ES rcp85_r1i1p1	MRI-CGCM3 rcp45_r1i1p1	CCSM4 rcp45_r2i1p1	CSIRO-Mk3-6-0 rcp85_r1i1p1
Percentile	n/a	n/a	10	50	90	10	50	90	10	50	90
ω_0	0.017202801	0.017202801	0.017202801	0.017202801	0.017214206	0.017214206	0.017214206	0.017453293	0.017202801	0.017214206	0.017214206
$a_{0,m}$	-4.8083E-05	-4.43368E-05	-1.96145E-05	-2.14059E-05	-5.58497E-05	-4.14661E-06	-1.54413E-06	-4.72936E-05	2.90642E-06	4.26283E-06	-4.69866E-05
$a_{0,b}$	17.23206333	17.03036043	16.2034187	15.42793085	15.13802901	15.99580841	15.06728682	13.08018038	14.91161659	14.09603103	12.49022375
a_1	15.23213492	14.73219684	14.83754411	14.67150206	14.43762213	14.83603732	14.69045788	13.61506775	14.54181886	14.74105908	12.82633108
b_1	3.342606183	3.220204015	3.718669408	3.529517529	3.336574996	3.419498941	3.620037228	3.110456889	3.997279091	3.200245624	3.629305941
a_2	1.468660625	1.464367154	1.10219893	1.454140072	1.054648829	1.018273816	0.892251463	1.149678521	1.382258831	1.195664621	1.077147249
b_2	-0.088406908	0.139786155	0.023892158	0.336360809	-0.378188957	-0.28122722	-0.169942549	0.151152019	0.464245082	-0.239144061	0.36861066
a_3	0.287517799	0.156739711	0.360015341	0.641591857	0.457508508	0.321954079	0.439915333	-0.093852812	0.506827125	0.589125327	0.163958455
b_3	0.067527865	-0.013519609	-0.155648453	0.493464399	-0.032825212	-0.133183196	-0.213896113	-0.339578995	0.108758158	-0.465430468	-0.044410808
a_4	-0.180162551	-0.101271764	-0.023724021	0.075898002	0.139768975	0.199418056	-0.418772906	0.331527502	0.037682412	-0.091715559	0.519941631
b_4	-0.119631061	-0.027828816	0.256887665	0.263847685	0.62228101	-0.005199677	0.336684908	-0.016072796	0.313540148	0.436197207	0.456370355
R^2	0.745	0.728	0.771	0.76	0.774	0.752	0.756	0.743	0.775	0.775	0.78
HDD_{norm}	6198	6132	5880	5593	5414	5830	5496	4617	5452	5154	4465
a_{max}	0.009343367	0.009187556	0.009368555	0.009449812	0.010754866	0.011129715	0.004382237	0.023524204	0.005914476	0.014441362	0.014932445
b_{max}	-0.028277915	-0.017321229	-0.030195839	-0.02423774	-0.03839849	-0.061709718	0.191527833	-0.380402357	0.005914476	0.014441362	0.014932445
c_{max}	0.743114068	0.537067926	0.666322265	0.614770717	0.703215109	2.897370214	1.663706694	2.985818857	0.005914476	0.014441362	0.014932445
a_{min}	-0.024757734	-0.028764403	-0.019707953	-0.017713971	-0.020790255	-0.011394747	-0.010143071	-0.033095768	-0.013528679	-0.027737215	-0.015002573
b_{min}	0.635328965	0.738107588	0.445743682	0.389968668	0.440196511	-0.023517781	-0.182094323	0.618816937	-0.013528679	-0.027737215	-0.015002573
c_{min}	-5.622372946	-6.098763854	-4.372258737	-4.066853179	-4.272169259	-2.842500316	-2.698462066	-4.418541482	-0.013528679	-0.027737215	-0.015002573
R_G^2	n/a	n/a	0.716	0.711	0.683	0.656	0.754	0.688	0.712	0.736	0.66
R_A^2	n/a	n/a	0.752	0.744	0.714	0.688	0.791	0.718	0.747	0.768	0.691

***Note: R_G^2 and R_A^2 are the R^2 coefficients for the models when fitted to the gridded historical data and the observed historical data, denoted by subscripts G and A respectively.**

Table 2 – Temperature Model Regression Coefficients

Model Coefficient	(1971-2000)	2030 (2011-2040)			2050 (2041-2070)			2080 (2071-2100)		
	Gridded	MRI-CGCM3 rcp26_r1i1p1	CNRM-CM5 rcp85_r1i1p1	CanESM2G rcp85_r1i1p1	GFDL-ESM2G rcp26_r1i1p1	CCSM4 rcp26_r2i1p1	HadGEM2-ES rcp85_r1i1p1	MRI-CGCM3 rcp45_r1i1p1	CCSM4 rcp45_r2i1p1	CSIRO-Mk3-6-0 rcp85_r1i1p1
Percentile		10	50	90	10	50	90	10	50	90
ω_0	0.017202801	0.017202801	0.017202801	0.017214206	0.017214206	0.017214206	0.017453293	0.017202801	0.017214206	0.017214206
$a_{0,m}$	4.90597E-05	1.97226E-05	8.42803E-05	6.17361E-05	4.39725E-06	6.45161E-06	5.84443E-05	-2.39407E-06	-3.41088E-06	5.12677E-05
$a_{0,b}$	-1.183511098	-0.110961913	-0.035348355	1.060269574	0.134099583	1.14431529	3.30908555	1.218783375	2.292497734	4.092586529
a_1	-15.32646713	-15.00483678	-15.01016522	-14.85889671	-15.07031772	-15.13043677	-14.38903323	-14.77511771	-15.46651812	-13.86442651
b_1	-3.373905148	-3.767462247	-3.617937893	-3.417473561	-3.486720669	-3.672134199	-3.398585429	-4.08314933	-3.273247832	-4.000847363
a_2	-1.399299696	-0.973277644	-1.190849709	-0.733668652	-0.853505842	-0.548661893	-0.676104008	-1.233816285	-0.627483518	-0.446974694
b_2	0.139715166	0.055066812	-0.175901094	0.503433466	0.383842067	0.251251196	0.280735201	-0.331933867	0.348026221	0.157410368
a_3	-0.316749491	-0.433384983	-0.805837843	-0.661299073	-0.409894843	-0.66371412	-0.066866833	-0.564850527	-0.963082798	-0.395529447
b_3	-0.120609428	0.074649882	-0.65838044	-0.083716295	0.036649112	0.14005645	-0.045717935	-0.234566112	0.369409517	-0.375125428
a_4	0.183917498	0.059725938	0.014732396	-0.030763739	-0.16791805	0.538599982	-0.367785225	-0.046702552	0.291514309	-0.506207158
b_4	0.159168431	-0.197104656	-0.124195357	-0.548791787	0.069826391	-0.297660242	0.246987139	-0.230532276	-0.382978814	-0.264312534
R^2	0.745	0.772	0.761	0.777	0.754	0.76	0.752	0.776	0.782	0.786
$T_{avg,norm}$	-0.915829533	0.00	0.43	1.40	0.16	1.18	3.62	1.21	2.27	4.37
a_{max}	0.029577815	0.023475725	0.01742952	0.024563718	0.01426212	0.019010197	0.028818373	0.013494023	0.015781136	0.024331757
b_{max}	-0.111521367	-0.136723131	-0.111990575	-0.172663283	-0.367182038	-0.384027895	-0.424185377	-0.169714999	-0.408918963	-0.352342095
c_{max}	1.396640031	2.107959909	2.088663328	2.212868867	5.70737891	4.775071265	3.124590345	2.60492558	6.366232116	3.112610155
a_{min}	-0.022428303	-0.020978286	-0.018008224	-0.017695542	-0.017435903	-0.016968822	-0.025263233	-0.017582627	-0.011439714	-0.020361897
b_{min}	0.122344611	0.160479492	0.166812133	0.200826456	0.24285824	0.268864804	0.348017561	0.151651082	0.262476194	0.25496514
c_{min}	-1.856017883	-1.884867345	-2.584833819	-2.497314327	-4.44882885	-3.931077304	-2.902387715	-2.013196881	-5.229527819	-2.746372471
R_G^2	n/a	0.723	0.724	0.714	0.727	0.755	0.737	0.739	0.819	0.749
R_A^2	n/a	n/a	n/a	n/a	n/a	n/a	n/a	n/a	n/a	n/a

***Note: R_G^2 and R_A^2 are the R^2 coefficients for the models when fitted to the gridded historical data and the observed historical data, denoted by subscripts G and A respectively.**

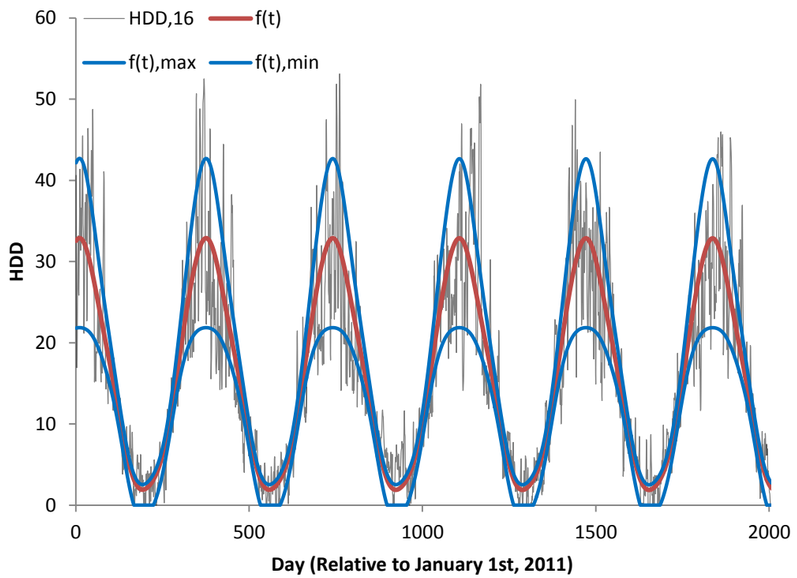

Figure 1 – 2030 Normal: MRI-CGCM3 HDD

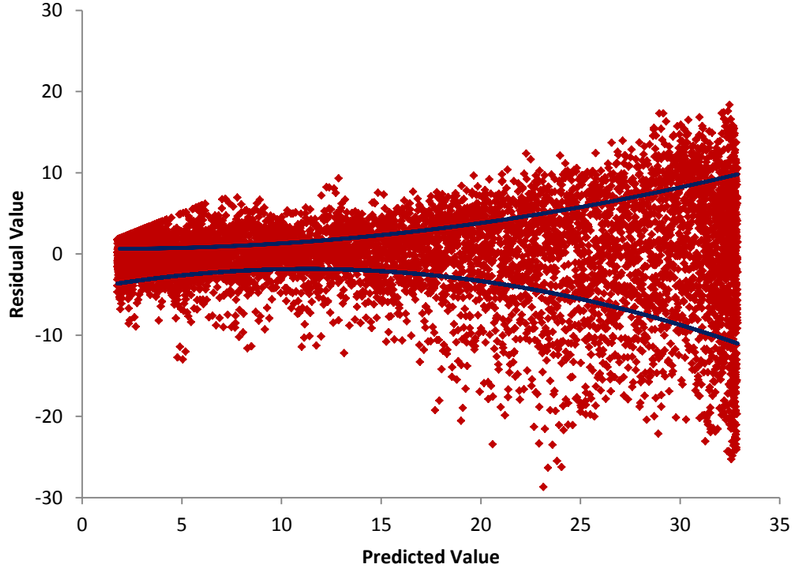

Figure 2 – 2030 Normal: MRI-CGCM3 HDD Residuals

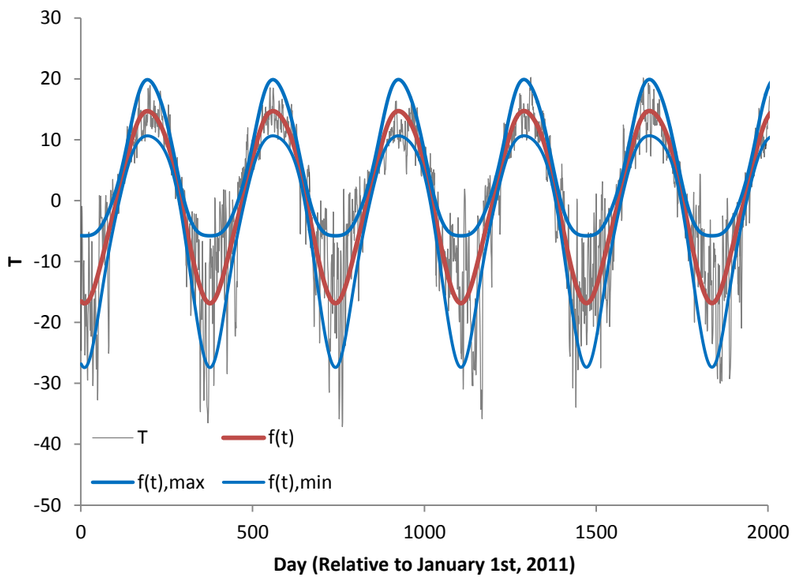

Figure 3 – 2030 Normal: MRI-CGCM3 Temperature

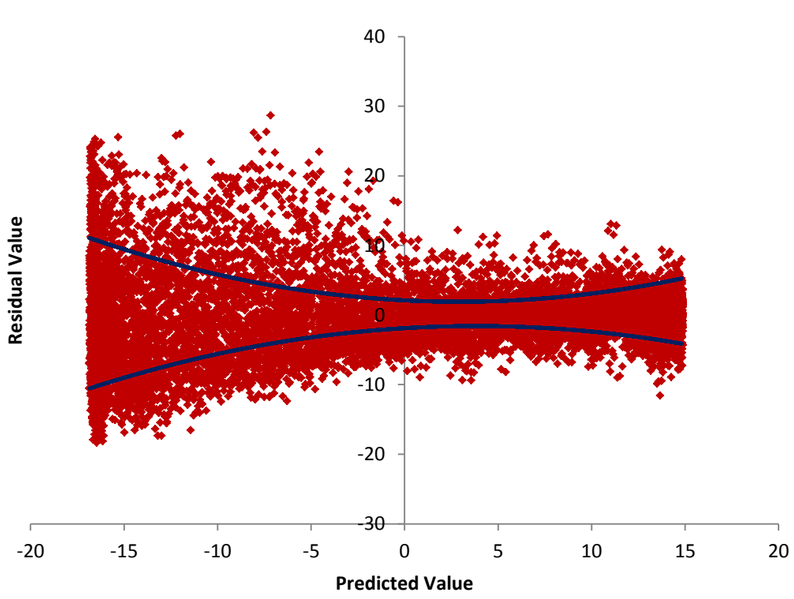

Figure 4 – 2030 Normal: MRI-CGCM Temperature Residuals

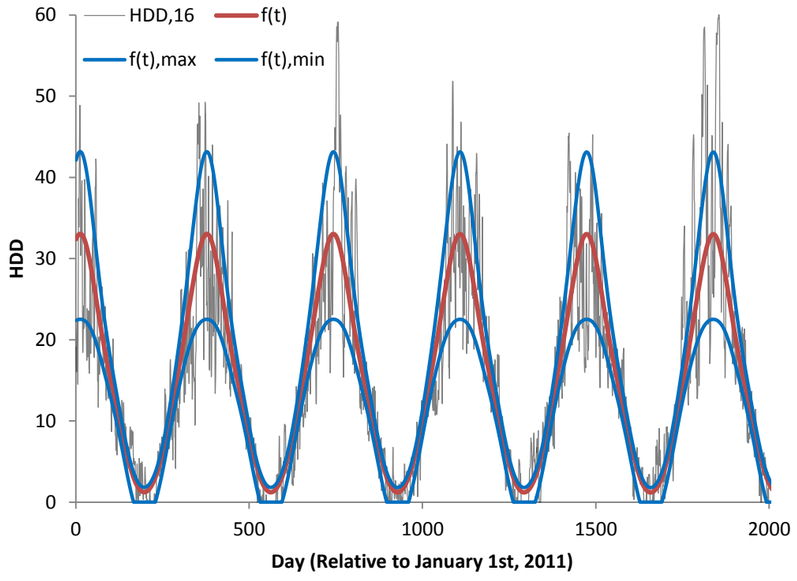

Figure 5 – 2030 Normal: CNRM-CM5 HDD

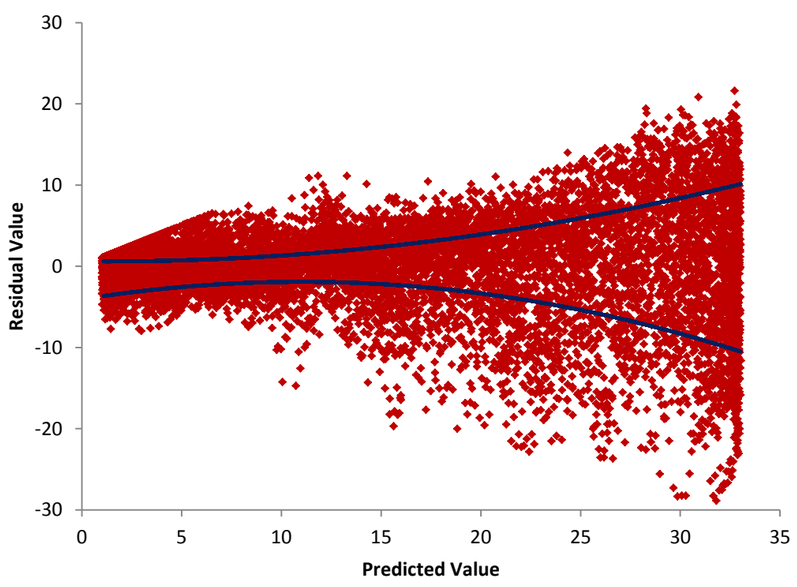

Figure 6 – 2030 Normal: CNRM-CM5 HDD Residuals

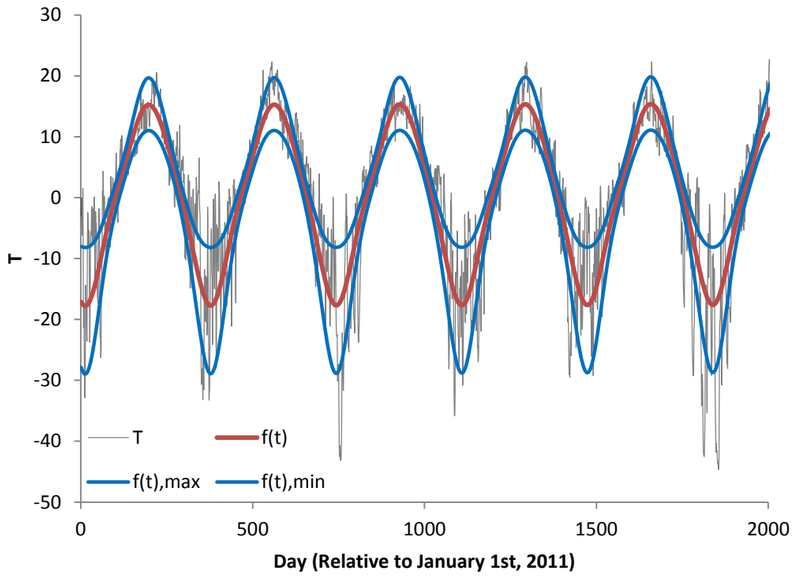

Figure 7 – 2030 Normal: CNRM-CM5 Temperature

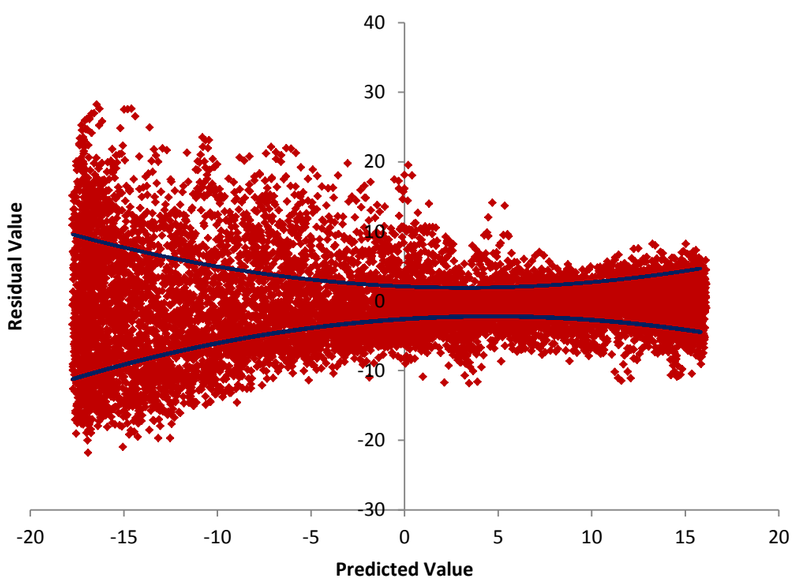

Figure 8 – 2030 Normal: CNRM-CM5 Temperature Residuals

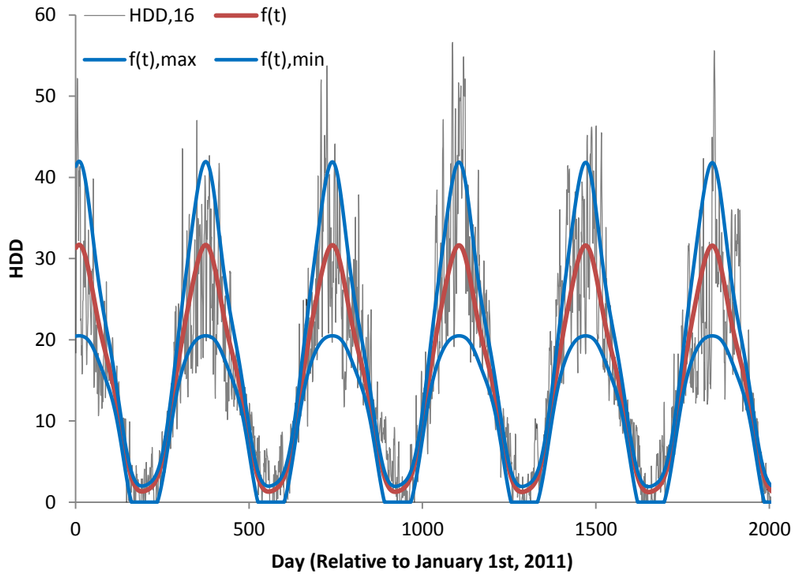

Figure 9 – 2030 Normal: CanESM2G HDD

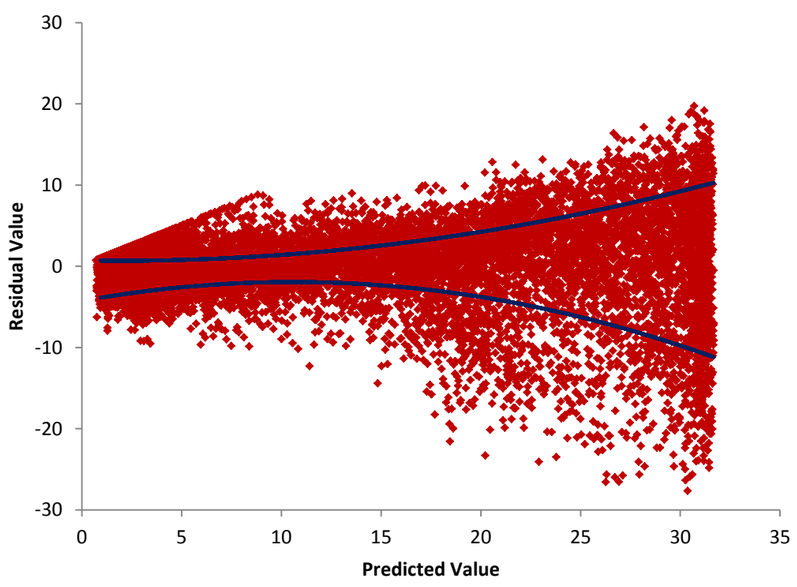

Figure 10 – 2030 Normal: CanESM2G HDD Residuals

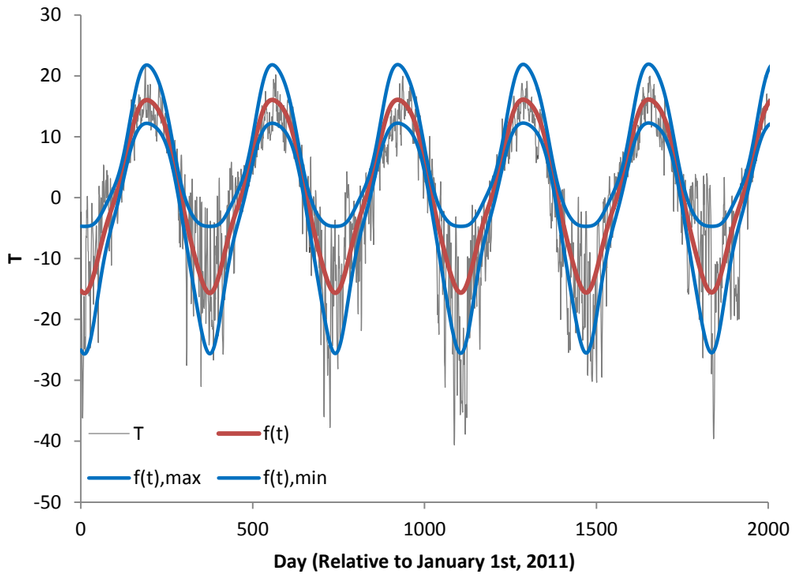

Figure 11 – 2030 Normal: CanESM2G Temperature

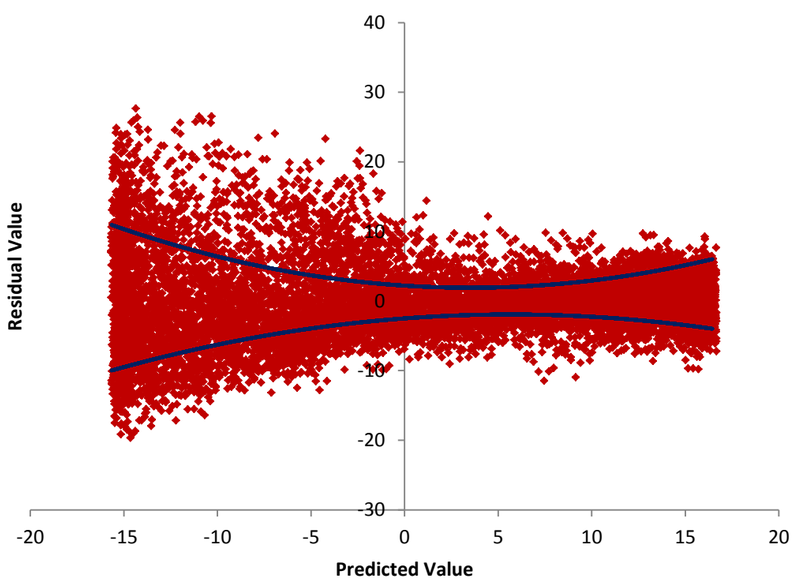

Figure 12 – 2030 Normal: CanESM2G Temperature Residuals

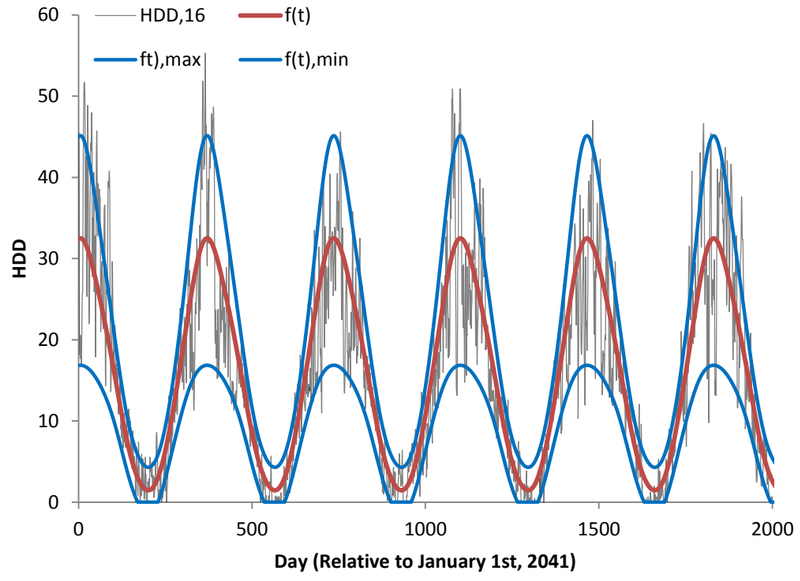

Figure 13 – 2050 Normal: GFDL-ESM2G HDD

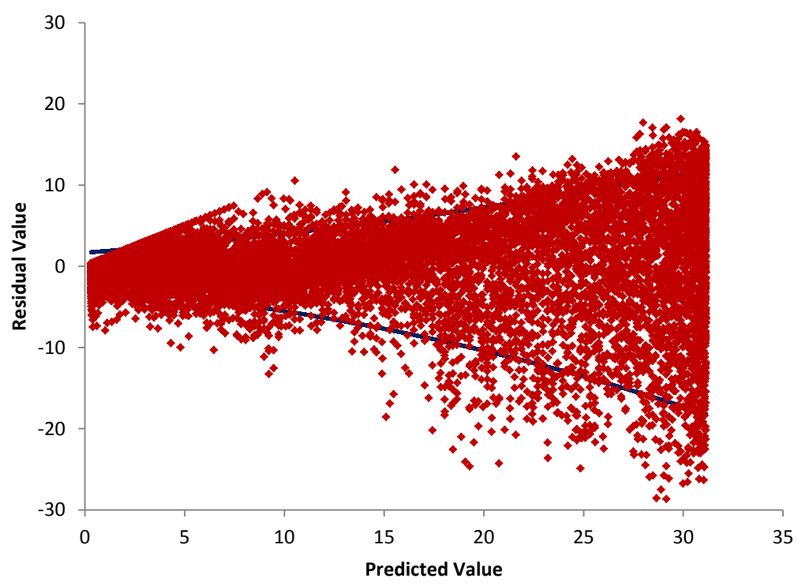

Figure 14 – 2050 Normal: GFDL-ESM2G HDD Residuals

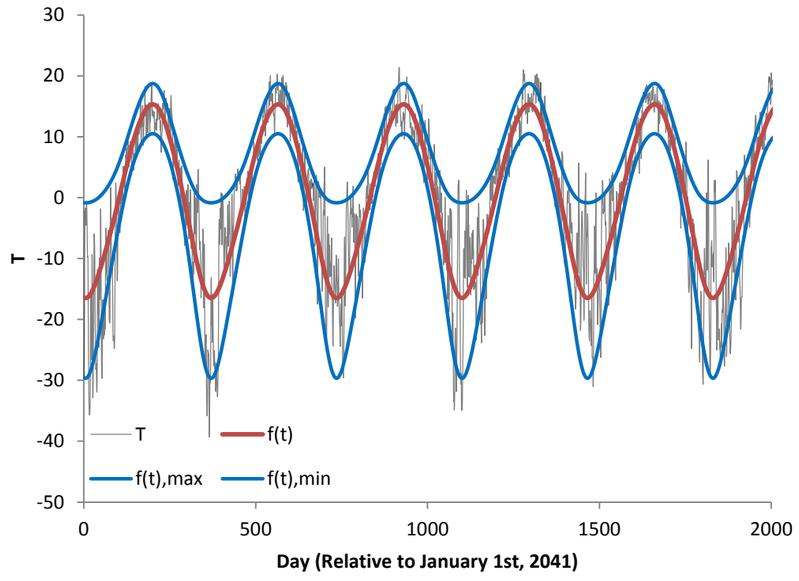

Figure 15 – 2050 Normal: GFDL-ESM2G Temperature

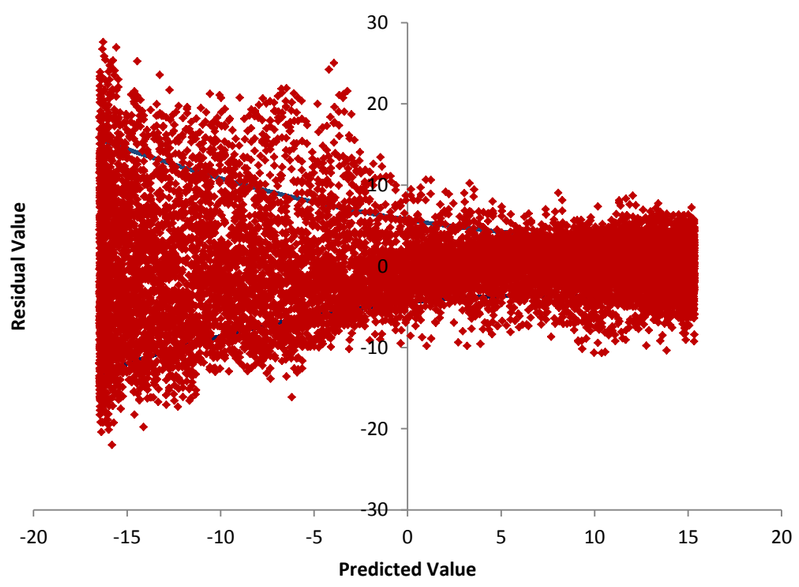

Figure 16 – 2050 Normal: GFDL-ESM2G Temperature Residuals

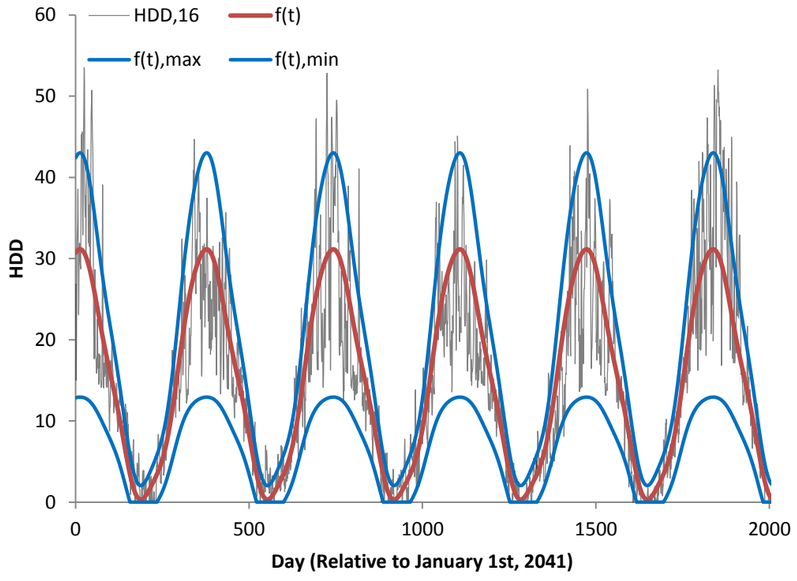

Figure 17 – 2050 Normal: CCSM4 HDD

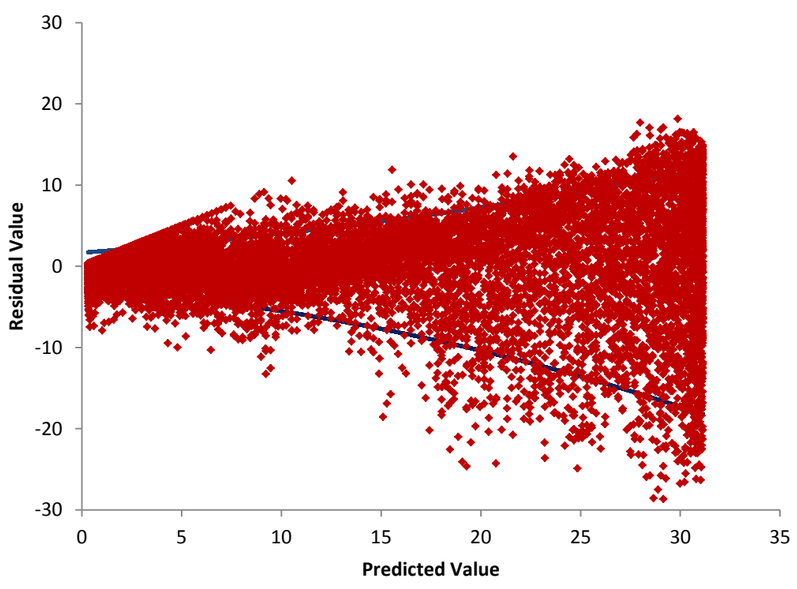

Figure 18 – 2050 Normal: CCSM4 HDD Residuals

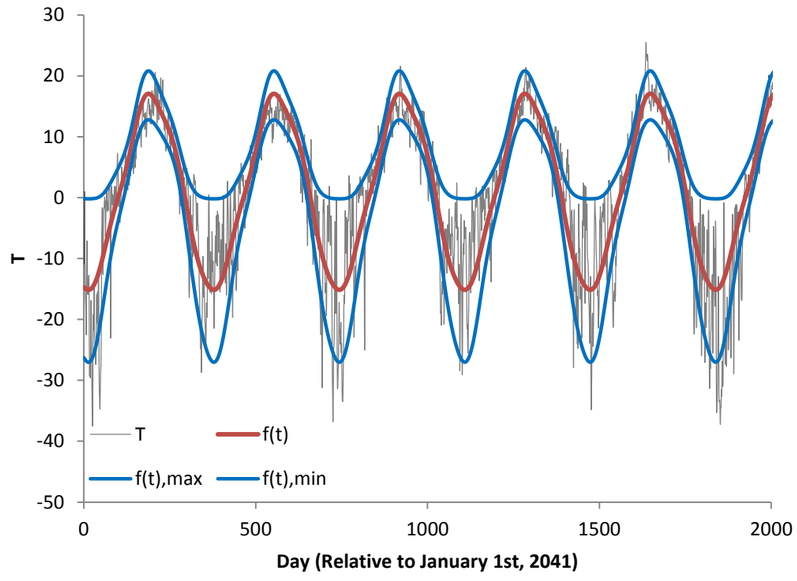

Figure 19 – 2050 Normal: CCSM4 Temperature

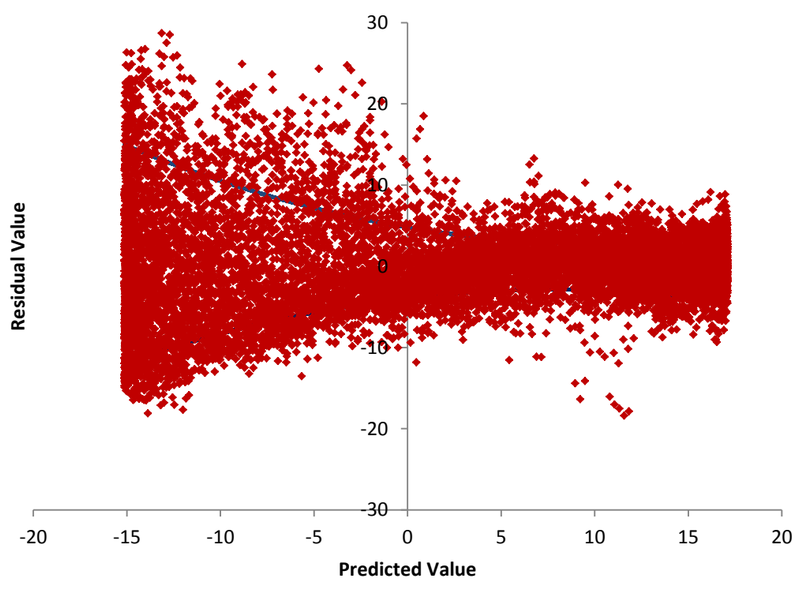

Figure 20 – 2050 Normal: CCSM4 Temperature Residuals

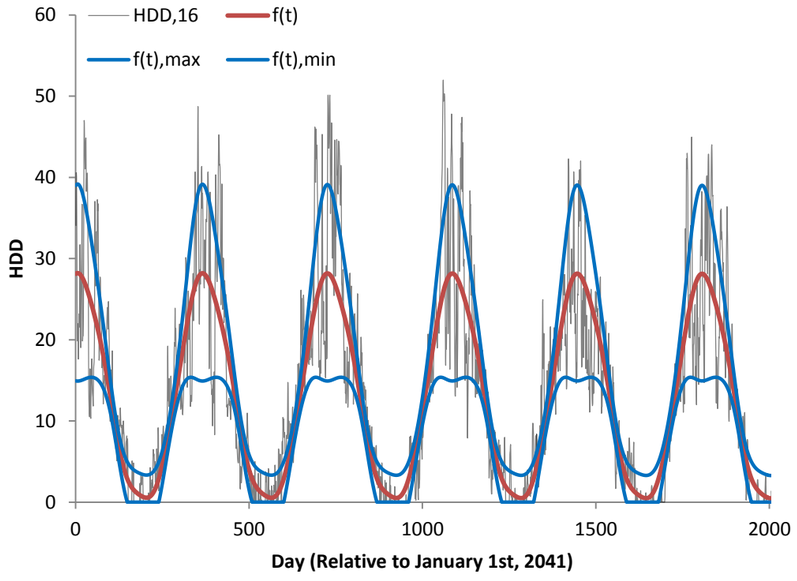

Figure 21 – 2050 Normal: HadGEM2-ES HDD

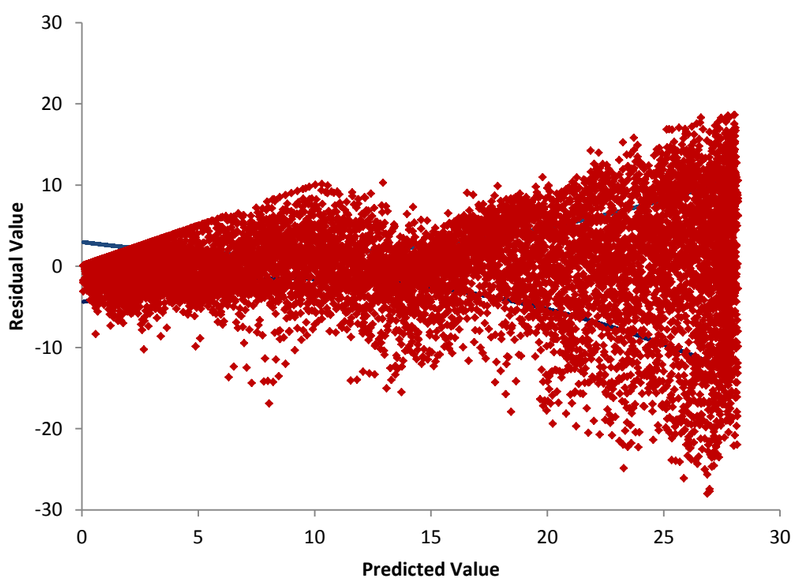

Figure 22 – 2050 Normal: HadGEM2-ES HDD Residuals

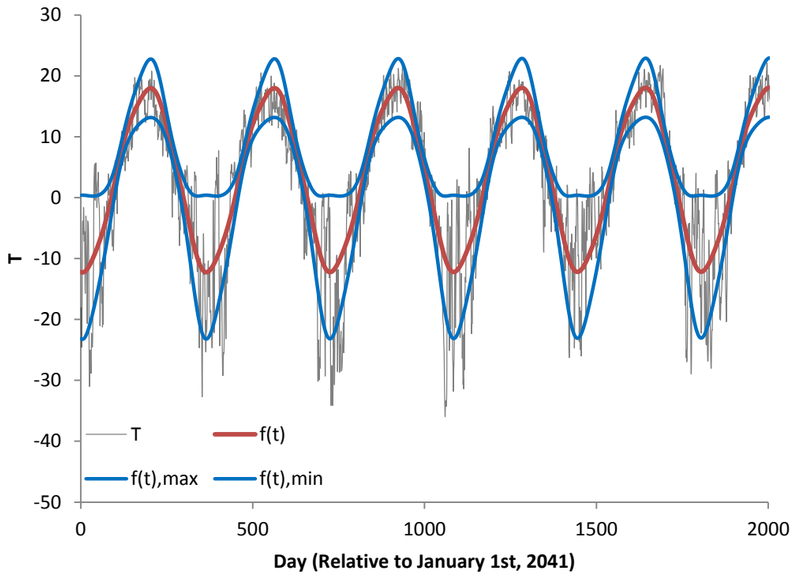

Figure 23 – 2050 Normal: HadGEM2-ES Temperature

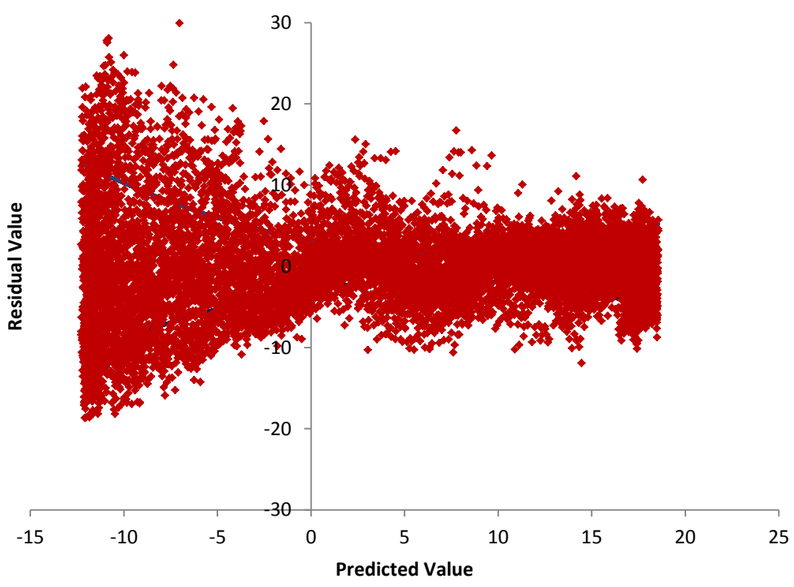

Figure 24 – 2050 Normal: HadGEM2-ES Temperature Residuals

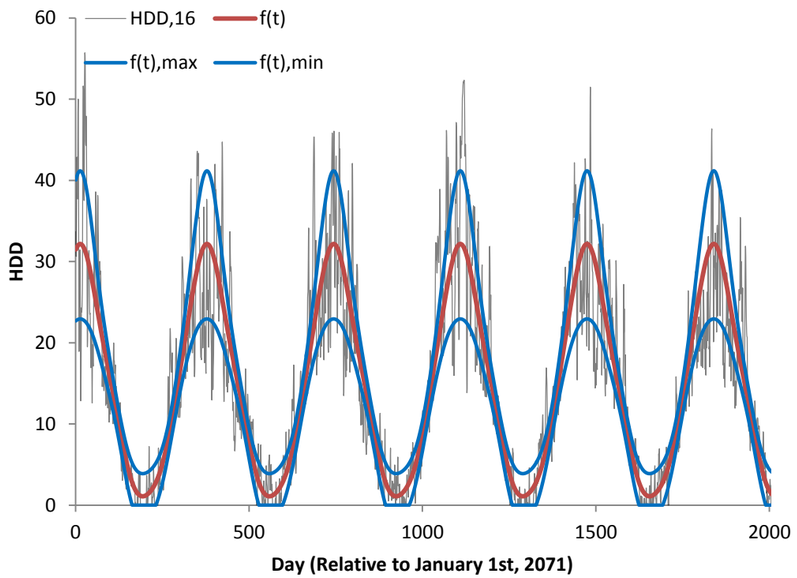

Figure 25 – 2080 Normal: MRI-CGCM3 HDD

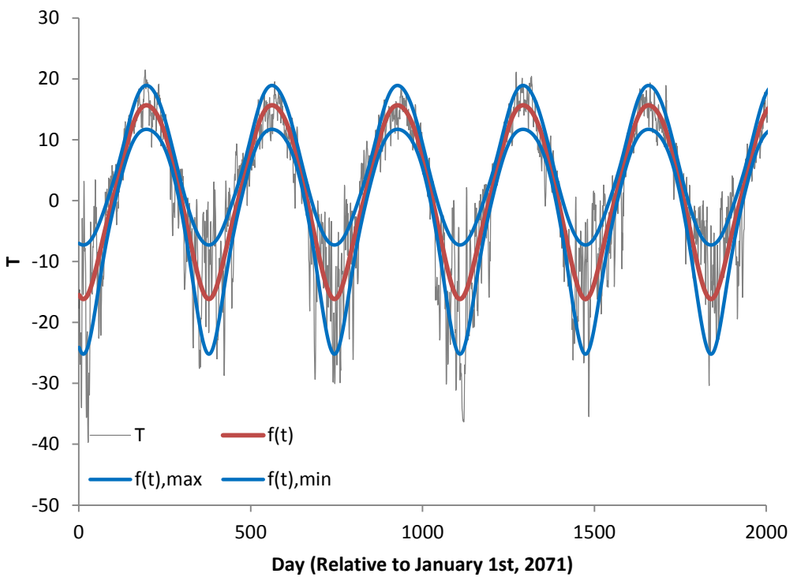

Figure 27 – 2080 Normal: MRI-CGCM Temperature

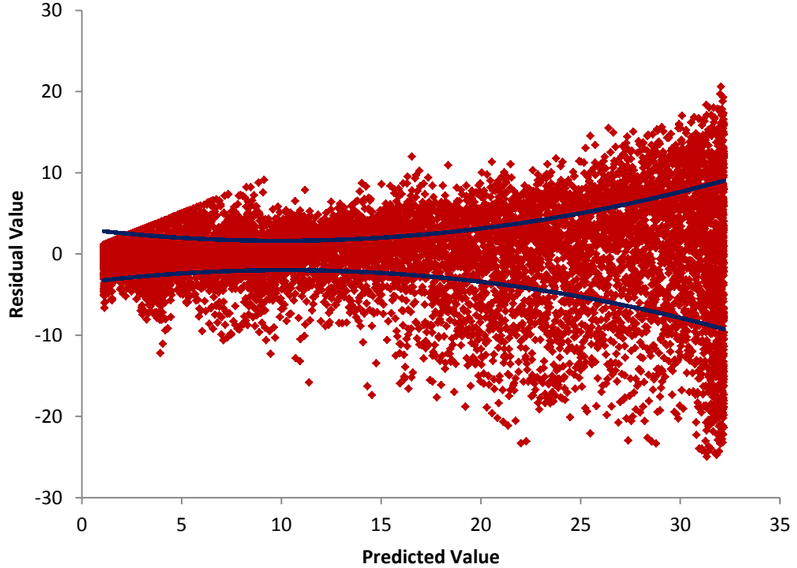

Figure 26 – 2080 Normal: MRI-CGCM3 HDD Residuals

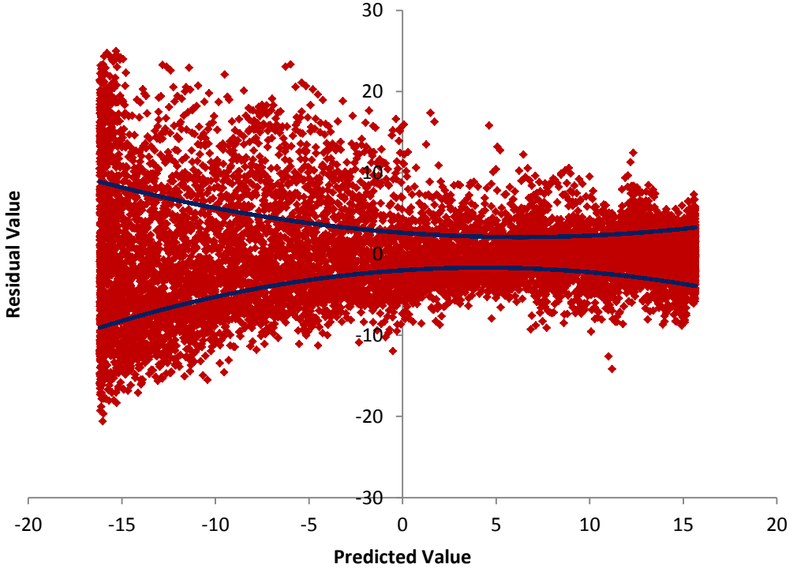

Figure 28 – 2080 Normal: MRI-CGCM3 Temperature Residuals

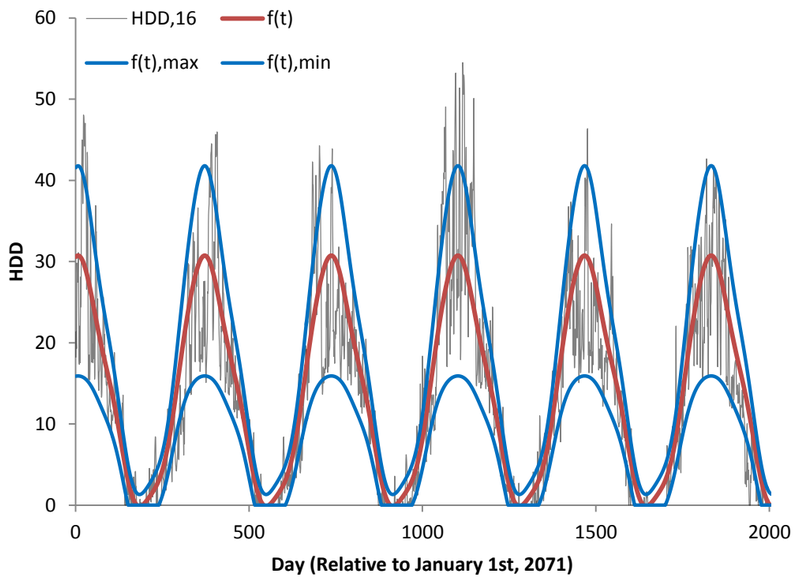

Figure 29 – 2080 Normal: CCSM4 HDD

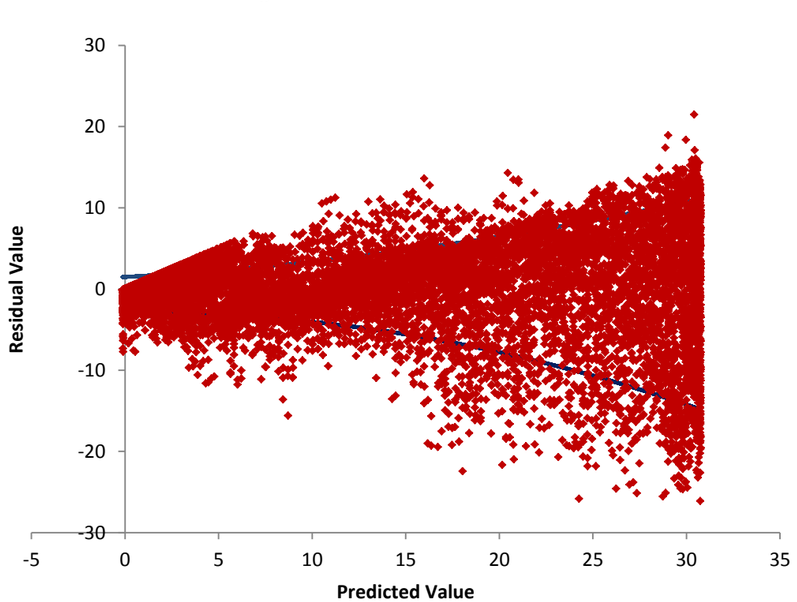

Figure 30 – 2080 Normal: CCSM4 HDD Residuals

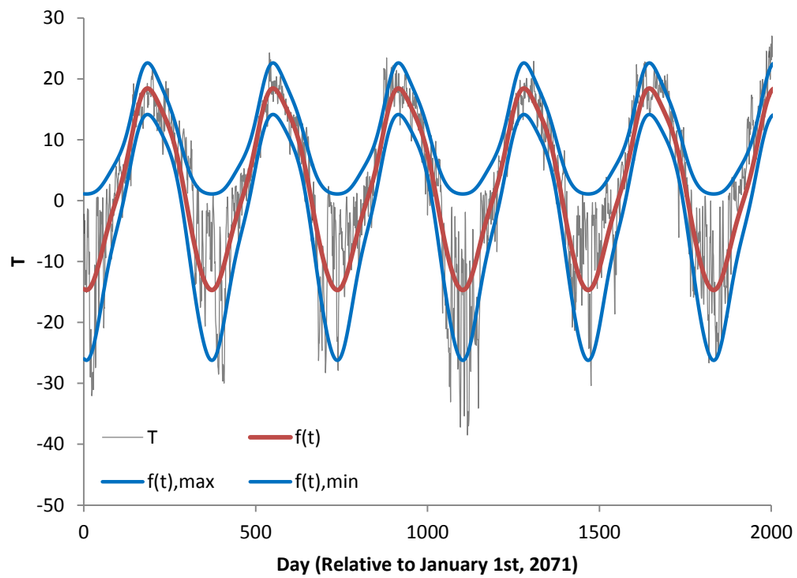

Figure 31 – 2080 Normal: CCSM4 Temperature

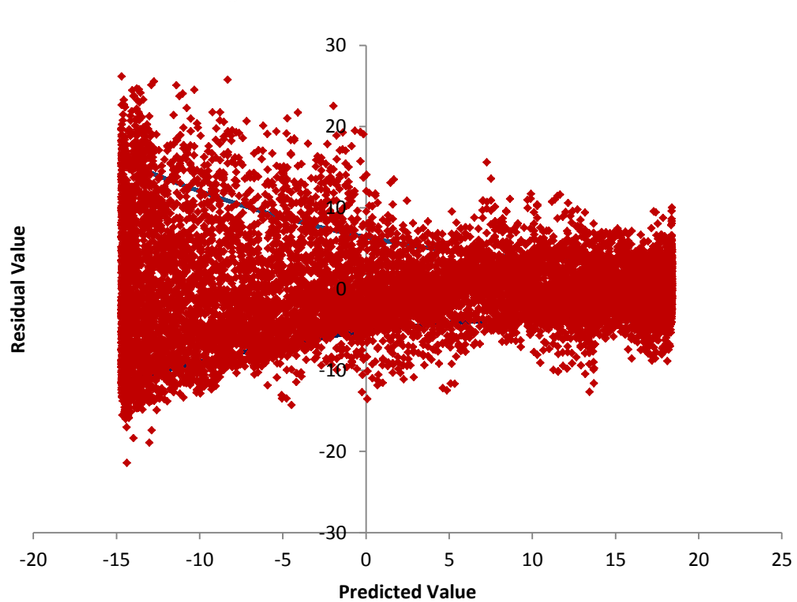

Figure 32 – 2080 Normal: CCSM4 Temperature Residuals

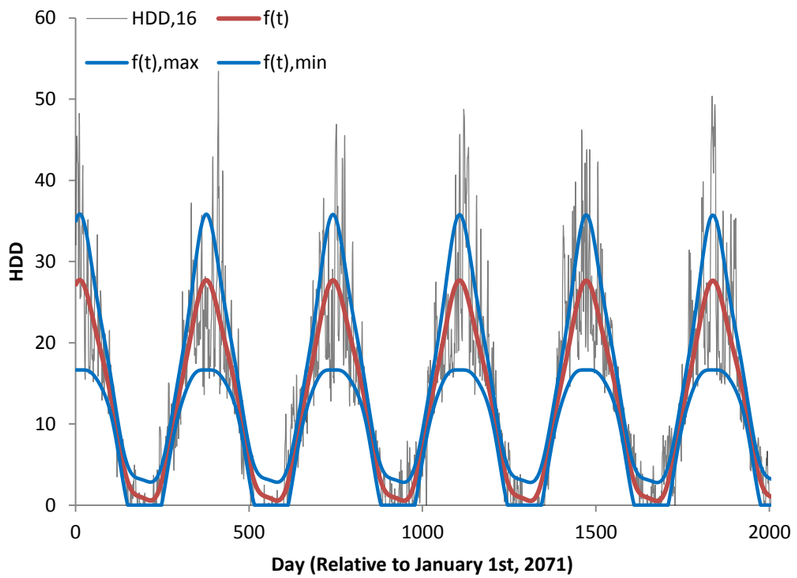

Figure 33 – 2080 Normal: CSIRO-Mk3-6-0 HDD

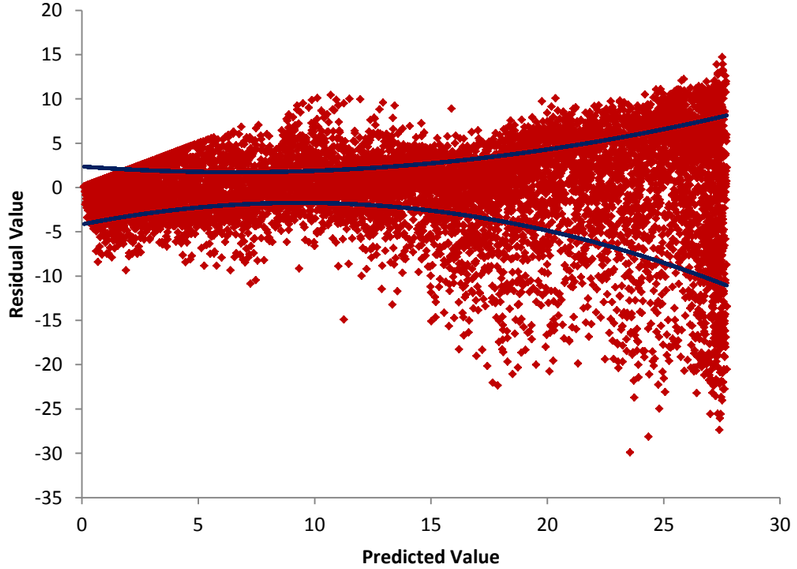

Figure 34 – 2080 Normal: CSIRO-Mk3-6-0 HDD Residuals

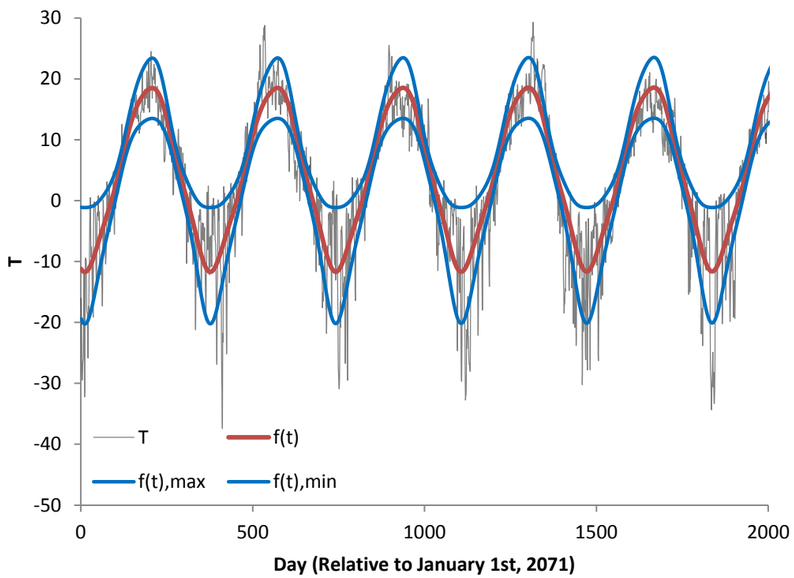

Figure 35 – 2080 Normal: CSIRO-Mk3-6-0 Temperature

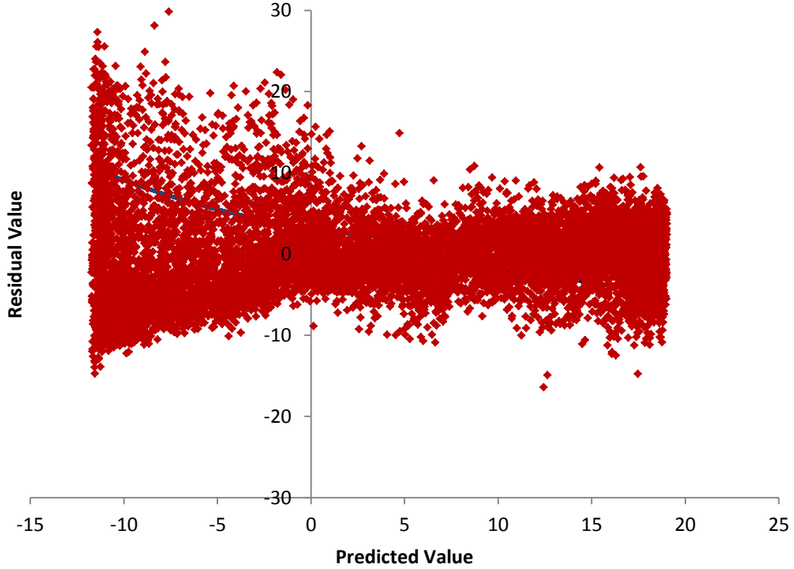

Figure 36 – 2080 Normal: CSIRO-Mk3-6-0 Temperature Residuals

Appendix A2 – Cooling Degree Day Model

Figure 37 to Figure 39 show cooling degree day data, calculated for a temperature of 20°C, for the selected 90th percentile climate models for the 2030, 2050, & 2080 climate normal periods. Qualitative assessment of the graphical representation of cooling degree day data for the three selected models reveals that the quantity of cooling degree days resulting from any model will be negligible in the short term, and increasing with time. However, the current energy model shows a negligible increase in description of past energy demand with the inclusion of cooling degree days (i.e. the vast majority of energy demand is described solely by heating degree days and the population). As such, cooling degree day data has been removed from further consideration of this study; however, the energy model will likely show an increase in correlation to cooling degree days in the future, at which time it will likely be necessary to review the impact of cooling degree days in future studies.

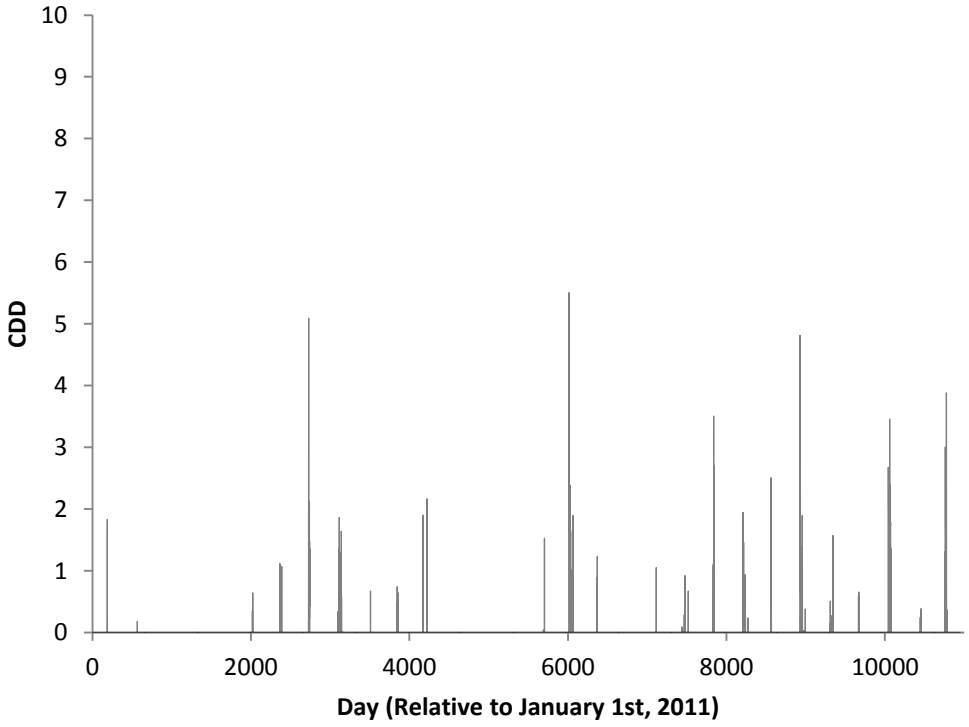

Figure 37 – 2030 Normal: CanESM2 CDD

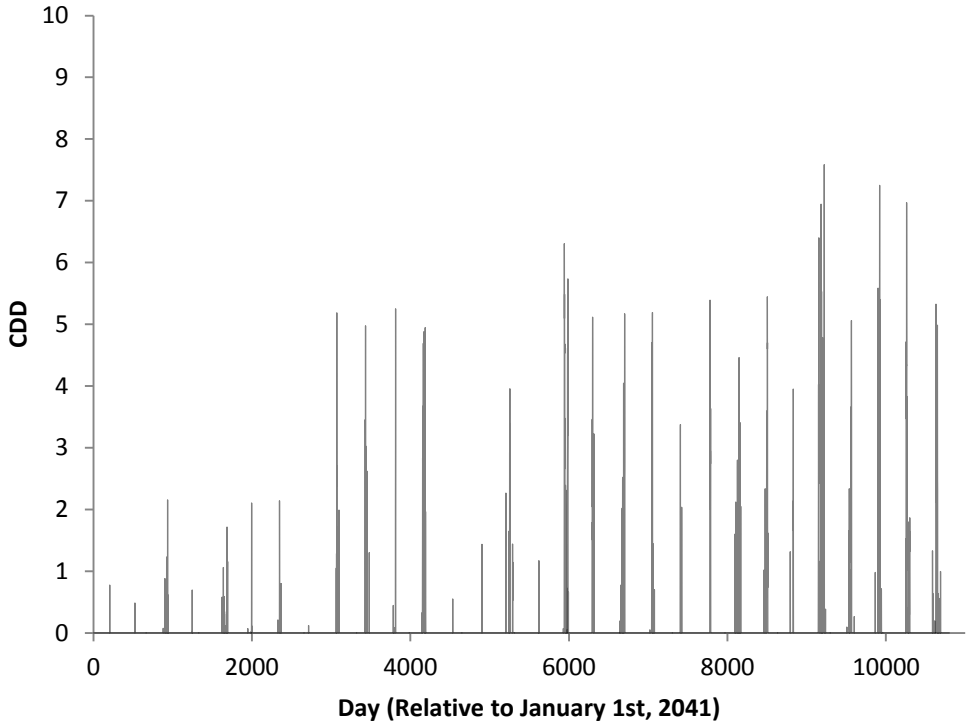

Figure 38 – 2050 Normal: HadGEM2-ES CDD

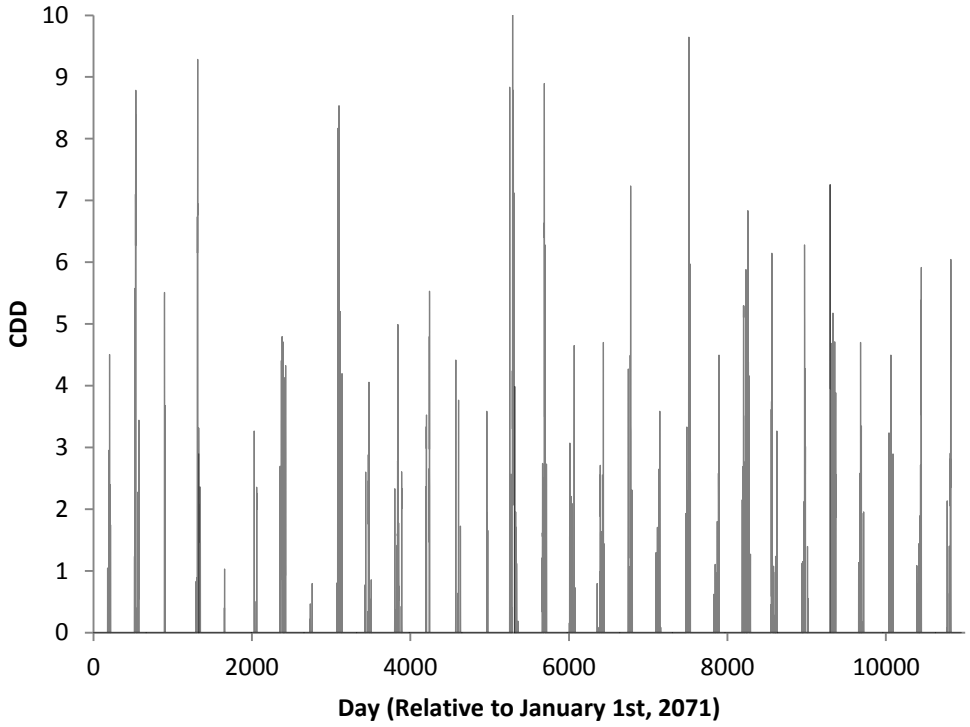

Figure 39 – 2080 Normal: CSIRO-Mk3-6-0 CDD

Appendix A3 – Population Model

The population models were determined from historical population data from March 1990 to December 2013, as obtained from Yukon Bureau of Statistics [3]. The data was used to determine four separate trends providing low, medium, high, and recent rates of linear increase. The models were then shifted to intersect with the final data point in the population data. Three scenarios were determined for use in the energy model, a constant, a low, and a high rate of increase. For this reason, the low and recent rates of increase were selected for use in determining the energy demand. Additionally, the populations were only modeled for the 2030 climate normal, as it is beyond the scope of this report to focus on the prediction of population changes beyond this timeframe. The population data and trends selected for use with the energy model are provided in Figure .

As can be seen, the differences between the three trends are substantial, with the average population for the 2030 normal being 27825, 29422, and 34955 for the constant, low rate of increase, and high rate of increase, respectively.

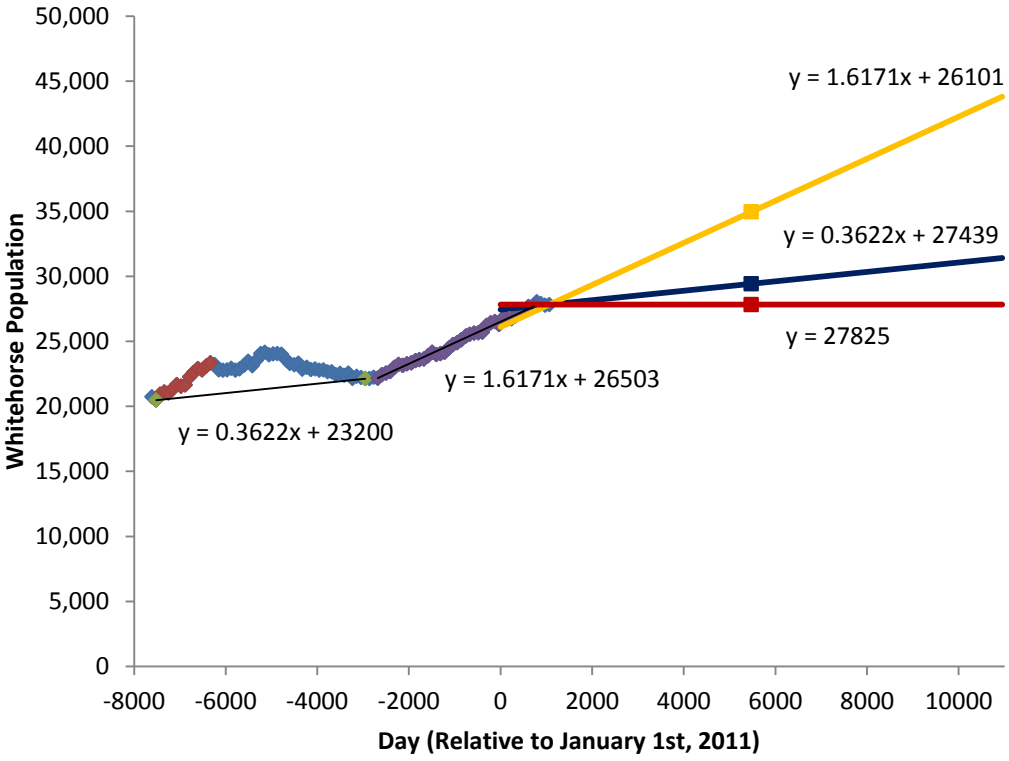

Figure 3 – Population Trends from 1990-2013 and 2040 Projections in Whitehorse, Yukon

Appendix A4 – Energy Model

The energy model is based on past data and is provided by YEC. The description of this model will be provided by YEC.

[Daily Load] = -1128.33692142593 + 14.0121566243262 * [HDD] + 0.0573731048045803 * [Population]
R2 = 91.52%

[Daily Load] = -1130.70690552463 + 14.0944264188271 * [HDD] + 2.16012691092298 * [CDD] + 0.0573848152605756 * [Population]
R2 = 91.53%

Appendix A5– Energy Demand

Energy demand was modeled using the provided heating degree day or temperature models, population models, and the energy model as provided in prior appendices. In the case of the temperature models, the daily heating degree days were calculated from the temperature model prior to use in the energy model. The populations were modeled as constant, a low rate of increase, and a high rate of increase for the 2030 normal, and only as constant for the 2050 & 2080 normals.

The resulting daily energy demands were then averaged for each model for each climate normal. By averaging the energy demands, the results of models with differing periods could be compared (i.e. to allow comparison between models with a 360, 365, or 365.242 day year). The results are provided in Table 3 for the heating degree day model and in Table 4 for the temperature model. The average daily energy demand can be seen to be nearly identical as determined with both the heating degree day model and temperature model, which is as expected. The results show two trends, an increase in energy demand as the rate of population growth increases and a decrease in energy demand with time. However, it is clear that even a low rate of increase in population results in a significantly larger increase in energy demand in comparison to the decrease of energy demand resulting from the increase in temperature (and thus the decrease in heating degree days).

Table 3 – Average Daily Energy Demand as Calculated from Heating Degree Day Models

Population Trend	Average Daily MWh (HDD Models)								
	2030 Normal			2050 Normal			2080 Normal		
	10th	50th	90th	10th	50th	90th	10th	50th	90th
Constant	694	683	676	692	679	648	677	666	639
Low Increase	785	774	768	n/a			n/a		
High Increase	1103	1092	1085						

Table 4 – Average Daily Energy Demand as Calculated from Temperature Models

Population Trend	Average Daily MWh (Temp. Models)								
	2030 Normal			2050 Normal			2080 Normal		
	10th	50th	90th	10th	50th	90th	10th	50th	90th
Constant	692	686	673	690	677	645	675	664	636
Low Increase	784	778	765	n/a			n/a		
High Increase	1102	1096	1082						

Appendix A6 – Data Deficiencies

Historical climate data is available from 1953 to present for Whitehorse, and is nearly 100% complete. There appears to be considerable variation between the OURANOS gridded data and the observed data.

There is no developed baseline from which it is possible to determine any varying trends in both efficiency and saturation of energy uses. The most important aspect of this is the “supposed” trend towards an increase in the use of electrical heat, which has the potential to have a significant effect on energy demand given the importance of heating on energy demand. The varying reports and information on energy use refer to surveys and studies that are either incomplete, or do not provide data that can be seen as applicable to the Yukon. There is also no breakdown of energy end use, which would be required to determine what proportion of energy use is actually relevant to the impacts of climate change.